Steam Purity Troubleshooting: The Berlin Geothermal Steam Field, El Salvador

Cristo Umanzor [1]*, Sadiq J. Zarrouk [1], and Aníbal Rodríguez [2]

[1]Department of Engineering Science, The University of Auckland, Private Bag 92019, Auckland, New Zealand

[2] LaGeo S.A. de C.V., 15 11.5 Carretera al Puerto de La Libertad, San Salvador, El Salvador

*cuma001@aucklanduni.ac.nz

Keywords: *Steam Purity, Berlin Geothermal Steamfield, El Salvador, Steam Scrubbing.*

ABSTRACT

Moisture carried with the geothermal steam at the turbine inlet can cause millions of dollars lost in electricity generation. These revenue losses occur due to frequent power plant overhauls, retrofitting and extended turbine maintenance required to remove the scaling out of the turbine blades and diaphragm or replace expensive turbine components (e.g. turbine shaft) damaged by entrained liquid droplets impacting the surfaces at high velocity.

Several technical articles, published since the onset of the geothermal industry, describe practical design techniques and recommendations to improve the steam field design effectiveness, to deliver dry and clean steam to the turbine. These criteria fundamentally refer to primary separation efficiency and steam line scrubbing (or secondary separation). Some of the design recommendations might be valid within a range of physical conditions (e.g. steam pressure or velocity) or applicable only to a specific steam field configuration. The authors consider an opportunity to combine all the design techniques, criteria, and experiences published to date into an integrated thermofluid model to either validate the well-known recommendations or optimise their results.

The Berlin Geothermal Steamfield (El Salvador) is presently experiencing problems with one of its turbine units due to impurities carried by the steam. LaGeo and the University of Auckland are working together to analyse the problem, develop and calibrate a model to simulate the current steam field, and assess optimisation scenarios to mitigate the steam purity problem.

This paper presents the findings, modelling results, and provide recommendations.

1. INTRODUCTION

1.1 Berlin Power Station and Steamfield Configuration

The Berlin geothermal steamfield is in El Salvador (Central America), around 112 km to the East of San Salvador city. Berlin is a two-phase medium enthalpy reservoir with 16 production wells, 21 reinjection wells, and five separation stations. The steamfield feeds a 109.4 MWe power station with four units, as listed in Table 1. It is important to note that U1 and U2 have been in continuous service for 22 years, with periodic overhauls scheduled every two years.

Most of the separation stations are installed at the production well pads, located uphill of the Tecapa volcano slopes and between 1.6 to 2 km away from the power station. The exception is TR-2/9 (the first installed separation station), located around 500m away from the power station steam collectors. The long distance between the separation stations and the power station should allow for good steam scrubbing and a high steam quality at the turbine inlets.

The staged steamfield development and drilling results justified the location of each of the existing separation stations. Figure 1 illustrates the steam gathering system configuration that feeds turbine unis U1 and U2.

Table 1: Berlin Power Station Turbine Units InformationUnits

Units	Capacity (MWe)	Plant Type	Comm. Year
U1	28.1	Single Flash	1999
U2	28.1	Single Flash	1999
U3	44.0	Single Flash	2007
U4	9.2	Binary	2007

Figure 1: Berlin Steamfield aerial view showing the three separation stations feeding U1 and U2 (Google Earth).

ISSN 2703-4275

1.2 Separation Systems

The primary separation is carried out by tangential inlet and Bottom Outlet Cyclone (BOC) separators located at the production well pads (Refer to Figure 2). The separated steam is conveyed to the power plan through relatively long cross-country steam lines (sizes DN500-750) provided with several condensate drain pots (CDP) and steam traps which, together with the power plant demisters, constitute the secondary separation system. Figure 3 shows the typical arrangement of the CDP and steam trap piping. The CDP's are typically DN300 diameter; the pot depth is 800mm with no internal baffle.

Figure 2: Separation Station at TR-4 Production well pad (see Figure 1)

Figure 3: Typical Condensate Drain Pot with Inverted Bucket Steam Trap Arrangement.

1.3 Steamfield Production

Table 2 summarises the average values of the main production parameters for each separator measured between 12 April and 23 May 2021. (LaGeo, 2021). This information is utilised as inputs for modelling purposes.

2. STEAM PURITY PROBLEMS AT U2

2.1 Steam Purity Monitoring

LaGeo frequently monitors the primary separation efficiency using chloride ion concentrations as a reference, and the average measured separation efficiency ranges between 99.444% to 99.999%. The chloride concentration measured at each separator is illustrated in Figure 4.

Table 2: Steamfield Production by Separators

Sep. ID	Wells	Press. (bar a)	Total (kg/s)	Steam (kg/s)	Enthalpy (kJ/kg)
TR-2/9	2	9.9	97.6	21.3	1,201
TR-4A	3	10.4	82.0	19.8	1,255
TR-4B	Off-line				
TR-5B	2	10.1	126.5	28.5	1,218
TR-5A	1	10.5	70.8	14.9	1,193
TR-5C	Off-line				
TR-17A	1	9.1	73.2	15.6	1,178
TR-17B	2	9.2	125.8	25.5	1,159
TR-18A	1	9.4	39.9	39.9	2,775
TR-18B	2	9.6	92.1	24.5	1,292

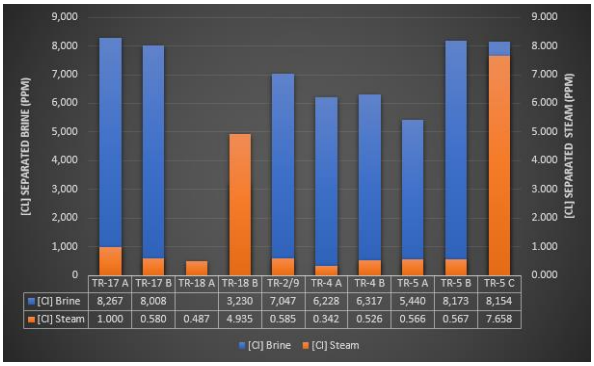

Figure 4: Chloride Concentration (ppm) in separated brine and steam

LaGeo maintains constant steam purity monitoring in the steamfield to track compliance with the minimum requirements set by the turbine manufacturer, which are listed in Table 3.

The measurements at the demister's outlet between 2018 and 2019 (LaGeo, 2019) shows that the supplier limits have not been exceeded during such period (Figure 5).

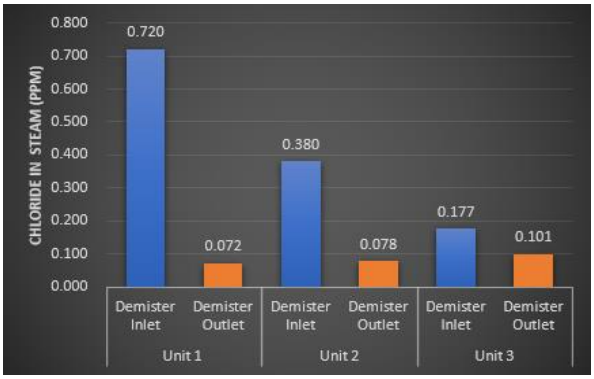

Figure 5: Average Chloride Concentration upstream and downstream of demisters.

Proceedings 43rd New Zealand Geothermal Workshop
23-25 November 2021
Wellington, New Zealand
ISSN 2703-4275

Table 3: Limit values recommended by the turbine manufacturer.

Steam Impurity	Recommended limits (ppm)
Total Dissolved Solids (TDS)	Less than five ppm
Chloride (Cl^-)	Less than one ppm
Silica (SiO_2)	Less than one ppm
Ion (Fe)	Less than one ppm

2.2 Startup Problems with U2

During the scheduled overhaul of U1 in March 2021, the routine test included the shutdown of all the power station units to inspect the substation conditions. After this test, U2 could not be put back online due to an abnormal free rotation obstruction. The O&M team removed the turbine cover to inspect the internal turbine components in detail and discovered significant mineral deposits in the rotor seals. Figures 6 and 7 illustrate the deposits found. Interestingly, the turbine blades and nozzles did not show substantial scaling problems. U2 overhaul occurred in January 2020. A similar event occurred a few years ago in the same U2, which contrasts with the reliable operation of U1 and U3, which have not experienced problems due to scaling or mineral deposits.

Figure 6: Mineral Deposits in Rotor Seal Grooves - Overall View

Figure 7: Mineral Deposits in Rotor Seal Grooves - Close View.

3. MODEL DESCRIPTION

3.1 Model Configuration

A new thermofluid model was developed to analyse the current steam gathering system's separation efficiency and explore solution options. The model focussed on the separation stations TR4 and TR-2/9, which feeds U2.

The model consists of the processes as follows:

- Primary separation efficiency (Lazalde-Crabtree, 1984),
- Calculation of thermodynamical properties upstream and downstream of each process block according to IAPWS IF-97 (Holmgren, n.d.).
- Mass balance for the steam, brine carryover and chloride flux from the cyclone separator outlets to the power plant steam collectors (Mills & Lovelock, 2020),
- Pressure drop through pipe and fittings (Rennels & Hudson, 2012),
- Heat losses across the steam lines (ASTM C680-19, 2019), and
- The separation efficiency of condensate drain pots (Lee, 1980),

The model is developed in Microsoft Excel, using arrays for data management and routine blocks for every process using Visual Basic Applications (VBA).

Figure 1 illustrates the physical arrangement on-site, and Figure 8 shows a simplified configuration.

Proceedings 43rd New Zealand Geothermal Workshop
23-25 November 2021
Wellington, New Zealand
ISSN 2703-4275

The model can also simulate scenarios varying critical process parameters like the one shown in Figure 11, and the outputs can also be plotted automatically in a graphical way.

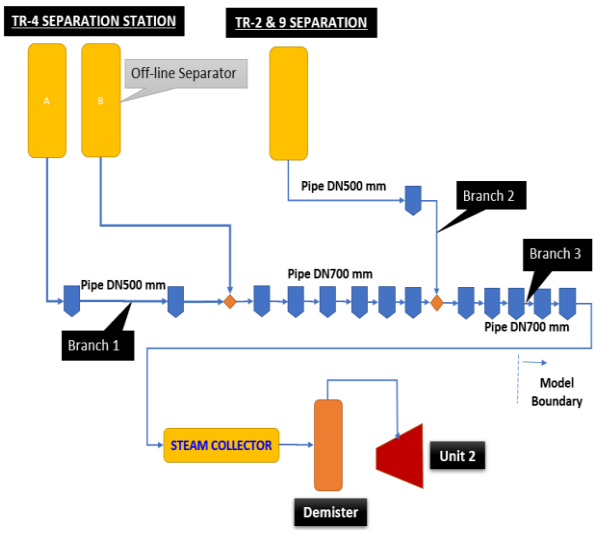

Figure 8: Simplified Model Configuration

3.2 Model inputs

The model analysed average production data such as wellhead pressures, separation pressures and flow rates obtained from the Daily Production Report (LaGeo, 2021) and between April and May 2021, which is the period with no significant operational changes.

The average chloride concentrations utilised in the simulation were gathered from the latest Separation Efficiency and Steam Purity Report (LaGeo, 2019).

Table 4 and Table 5 lists the main model inputs.

Table 4 – Production Data at the Separation Stations

Parameter	Separators	
	TR4A	TR-2/9
Separation Pressure (bar a)	10.4	9.9
Enthalpy (kJ/kg)	1,255	1,201
Mass Flow (kg/s)	82.0	97.6
Chloride in total flow (ppm)	4,724	5,508

Table 5 - General Model Inputs

Atmospheric pressure	0.94 bar a
Average Ambient Temperature	24 °C
External Wall Surface Temperature	60 °C
Wind speed	15 m/s
Insulation material	Calcium Silicate
Insulation Thickness	50 mm

4. MODEL RESULTS

4.1 Primary Separation Efficiency

Table 6 provides a comparison between the calculated separation efficiency and the measured efficiency based on chloride concentration. Marginal differences between the modelled and measured efficiencies are observed, and under the given operating conditions, the efficiency of the two separators is deemed high. However, these good separation efficiency values contrast with the mineral deposits found at the turbine.

Separator	Measured [Cl^-] base	Model	Diff (%)
TR-4A	99.9945%	99.9961%	0.16%
TR-2/9	99.9918%	99.9964%	0.46%

Table 6 - Separation Efficiency Comparison: Measured vs Model.

Figure 10 compares the main separator dimensions criteria proposed by Lazalde-Crabtree (1984) and the typical separator sizes for the type 350tph at Berlin, included in the model. In general, the overall key separator dimensions that significantly impact separation efficiency are close to the ones recommended by Lazalde-Crabtree (1984).

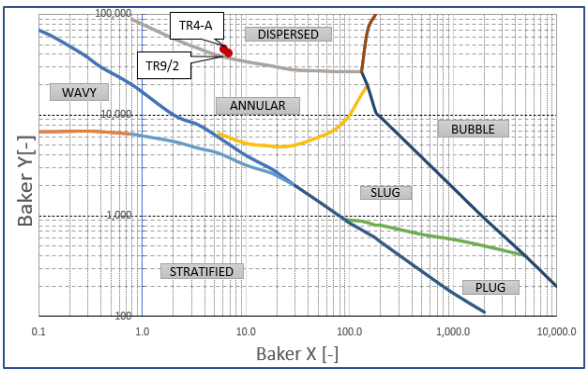

Figure 9 - Flow Regime at Two-Phase Inlet (Baker, 1954)

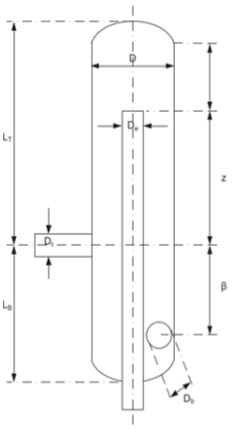

Lazalde-Crabtree (1984)

Parameter		Criteria		Berlin Sep. (350 tph)	Diff.
Inlet Pipe	Dt		-	470	-
Internal Diam.	D	3.3D_t	1,551	1,707	10%
Steam Outlet	De	1D_t	470	584	24%
Brine Outlet	Db	1D_t	470	363	-23%
Dim. Alpha	a	-0.15D_t	70	305	332%
Dim. Beta	b	3.5D_t	1,645	1,737	6%
Dim. Z	Z	5.5D_t	2,584	2,438	-6%
Dim. L_T	L_T	~6D_t	2,819	2,743	-3%
Dim. L_s	L_s	>4.0D_t	1,880	2,743	46%

Figure 10 - Berlin Separator Overall Size vs Lazalde-Crabtree Dimensions Criteria (Zarrouk & Purnanto, 2014)

Proceedings 43rd New Zealand Geothermal Workshop
23-25 November 2021
Wellington, New Zealand
ISSN 2703-4275

4.2 Secondary Separation Efficiency

The steam line from the separation station TR4A (Branch 1 in Figure 8) contains eight CDP's in series, and the pipe size after the fourth CPD changes from DN500 to DN700. The relatively small steam flow rate (19.8 kg/s) from the TR4A separator travels at low steam velocity (10.3 m/s) through the larger and longer pipe section, which should promote good carryover separation.

The steam line from the separation station TR-2/9 (Branch 2 in Figure 8) includes only one CDP (Named CDP90 in the model), which is an important feature because wells TR2 and TR9 together produce the highest chloride concentration (~7,047ppm in liquid phase) in the gathering system feeding U2. Figure 4 shows the different chloride concentrations in the steamfield.

The separation efficiency of the existing CDPs is unknown. However, a comparison between the dimensional ratios of the two existing typical sizes of CDP's installed along the TR-4 branch line and the CDP configuration tested by Lee (1980) indicates that the separation efficiency should be near 50%.

It is important to note that this simplified approach does not consider the adequate location of each CDP along the steam line and the relatively small size of the CDP leg for the DN700 steam line.

Dimension ratios	Recommended by Lee (1980)	Steam line size (D.N.)	On-Site CDP's
D/d	1.5	500	1.6
		700	2.3
h/d	≥ 1.24	500	~1.67
		700	~2.68

Table 7: CDP Dimensional Ratios Comparison

The model was iterated four times considering constant separation efficiency for all the CDP's ranging between 50% to 20%, and the results are plotted in Figure 11, which shows the chloride concentration in total flow downstream of each CDP from the separation stations TR4A and TR-2/9 to the U2 steam collector.

The model results indicate that the expected chloride concentration in total flow near the power station (0.0148 to 0.179 ppm) should be well below the concentration measured at the demister inlet of 0.38 ppm. This indicates that the overall efficiency of the existing secondary separation system is deemed low.

It is also interesting to observe the concentration jump downstream of the CDP90, located at the TR-2/9 steam branch line (Branch 2, Figure 8). This drastic change indicates that the steam from the TR4 separation station, scrubbed adequately by the first four CDPs, is "messed" again by the high chloride concentration steam supplied by the separator TR-2/9. However, the total steam flow is "re-scrubbed" by the subsequent five steam traps downstream of the TR4 and TR-2/9 flows merger (Branch 3).

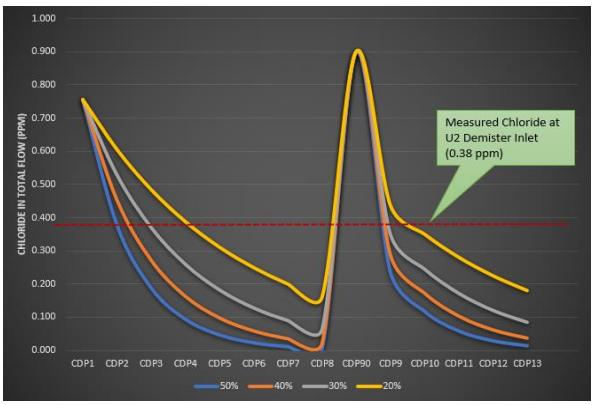

Figure 11 Chloride Concentration Upstream of U2 Demister vs Measured Value

4.3 Enhancement of First CDP downstream of TR-2/9

The chloride flow path through the steam lines can also describe the impact of CDP90 separation efficiency on the U2 steam purity detriment.

Based on the calculated primary separation efficiencies (See Table 6), the separated steam from TR-4A carries 14.9mg/s of chloride, while the steam from separator TR-2/9 adds 19.2 mg/s more to the U2 feeding lines. Assuming that the separation efficiency of the first eight CDP's from TR-4A is 50%, the chloride flux upstream of the merger with TR-2/9 flows should be less than 0.06 mg/s. This means that CDP90 and the remaining five CDP's downstream of the merger and upstream of the U2 steam collector need to evacuate fundamentally the chloride supplied by the TR-2/9 separator.

Figure 12 illustrates how the chloride flows are evacuated from the separator TR-4A to the U2 steam collector. The different curves downstream of the TR-4A and TR-2/9 merger shows the chloride removal with CDP90 operating at different separation efficiencies between 25% and 95%. Besides, Figure 12 shows that the most significant extraction of the chloride flow dissolved in the carryover occurs in the first CDP and steam trap arrangement downstream of the separator.

The above discussion means that the larger the separation efficiency at CDP90, the less chloride the U2 steam collector receives.

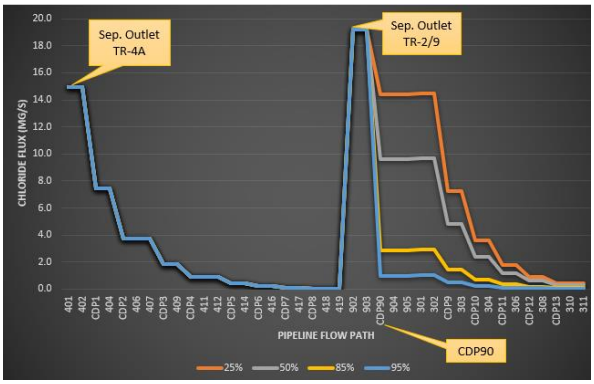

Figure 12 – CDP90 Efficiency Enhancement on U2 Steam Quality

Proceedings 43rd New Zealand Geothermal Workshop
23-25 November 2021
Wellington, New Zealand
ISSN 2703-4275

4.4 Heat Losses and Steam Condensate

The model results indicate that the condensation load produced due to heat transfer varies between 0.69 to 0.95 kg/h per meter of pipe. The average condensate load calculated in the model is slightly lower than the order of magnitude of 1 kg/h per meter reported by Morris (2015) and 0.9244 kg/hr per meter reported by Lee (1980). Such difference might be due to the higher average ambient temperature in Berlin compared to Wairakei.

The model was also executed twenty times, changing the thermal insulation thickness from 0 to 300 mm, using two different insulation materials (Calcium silicate and mineral fibre) and keeping the CDP's separation efficiency at 50%. Figure 13 shows the liquid flow rate at the U2 steam collector vs the thermal insulation thickness.

Given the current ambient conditions, assumptions and other model inputs, there is no significant reduction of the condensate loading by increasing the thermal insulation thickness beyond the current 50 mm thickness. In addition, the current condensate loading contributes to the chloride dilution and promotes steam scrubbing. However, the model ignores the condensate loading generated at startup conditions essential for adequate steam trap sizing.

The change in the insulation material from calcium silicate to mineral fibre also provides marginal improvement.

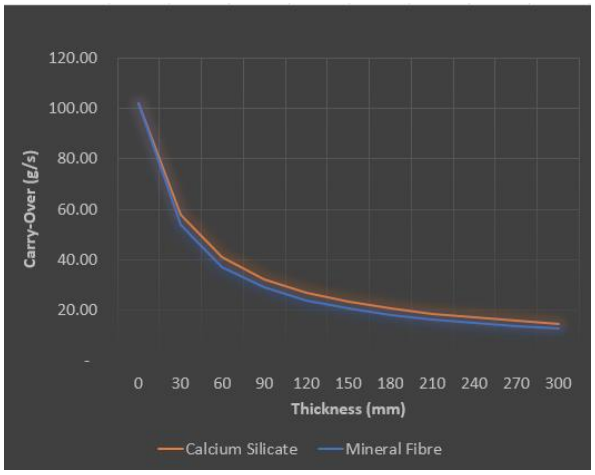

Figure 13: Carryover at U2 steam collector vs different thermal insulation materials and insulation thickness.

5. FAILURE ANALYSIS AND TROUBLESHOOTING

5.1 Improvement Opportunity

The total dissolved solids (TDS) in the steam supplied to U2 is 1.0 to 3.8 ppm (LaGeo, 2019). Considering a total steam flow rate of 41.1 kg/s, the mineral loading going into the turbine ranges between 148 to 562 g/h. These values contrast with recent publications based on experimental observations, which indicates that scaling should not be a significant problem if the mineral loading does not exceed 2 g/h (Morris, Mroczek, & Misa, 2019).

The assessment of the moisture removal above described and the U2 incident suggest an opportunity for improvement in the steam purity for the Berlin power station.

Figure 14 illustrates a simplified Failure Analysis and Troubleshooting (Bloch & Geitner, 1999) exercise to list the potential causes of the U2 startup failure.

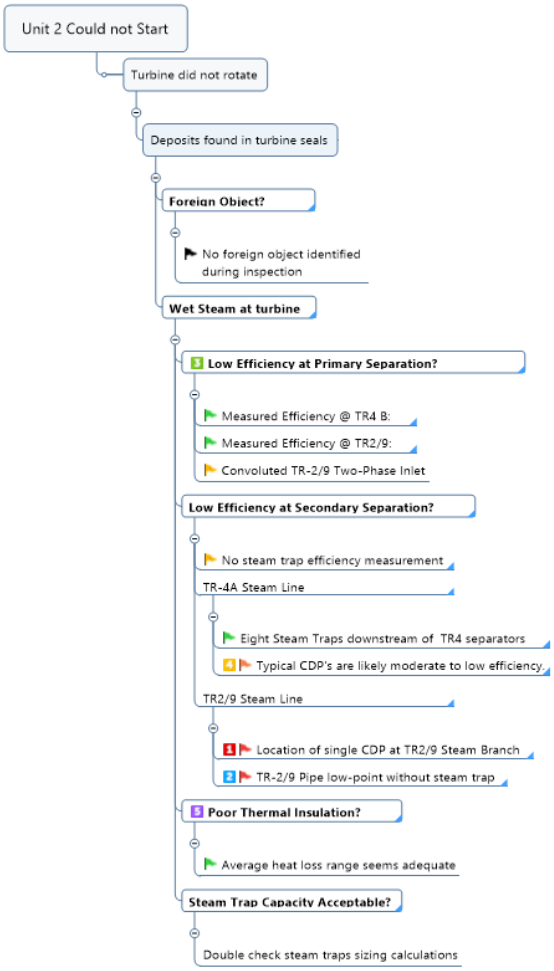

Figure 14: U2 - Failure Analysis And Troubleshooting Diagram

5.2 Potential Cause 1 – Poor efficiency of steam traps downstream of TR-2/9 join.

The only steam trap for the TR-2/9 steam branch line seems poorly located. The upward flow immediately upstream of the CPD may force the liquid droplets to flow over the CDP leg reducing their recollection. Jung (1995) recommends installing the CDPs away from bends and other fittings to avoid the turbulence shattering the liquid phase upstream of the steam trap.

This steam trap along the TR-2/9 branch line should be highly efficient because it is expected that the first CDP downstream of the separator should evacuate the most considerable portion of brine carryover. In addition, such high carryover from TR2/9 impacts TR-4A steam quality already scrubbed by the upstream CDP's.

5.3 Potential Cause 2: TR-2/9 steam line underground road crossing with no steam trap.

The existing steam branch line from TR-2/9 is not provided with a condensate removal device at the lowest point of the underground crossing. Hence, this arrangement is a

ISSN 2703-4275

permanent condensate pool which might affect the steam quality. The steam flow permanently drags the stagnant liquid pool increasing the carryover towards the power plant. This situation is also a significant safety and operational risk because it can cause a water hammer accident (Figure 15).

Figure 15 - TR-2/9 Steam Line and Road Crossing

5.4 Potential Cause 3: Poor Primary Separation Efficiency.

Based on current conditions, the measured values, and the model results, the primary separation efficiency for TR4A and TR-2/9 seems acceptable. However, the TR9 two-phase branch line connecting to the TR2 two-phase header seems very convoluted with several changes in direction, which promotes atomisation of liquid phase a few meters upstream of the separator inlet and may negatively impact the separation efficiency. See Figure 16 below.

Figure 16 - Two-Phase Inlet at TR-2/9 Separator

5.5 Potential Cause 4: Inadequate design of the CDP's of the DN700 steam header.

The diameter of the CDP's leg along the TR-4 main steam header seems relatively small (DN300) compared to the main steam line (DN700), potentially leading to low separation efficiency due to a small recollection area. In addition, the current CDPs do not have baffle plates which could improve the separation efficiency (Lee, 1980).

5.6 Potential Cause 5: Insufficient Thermal Insulation.

Assuming that the thermal insulation is well installed and dry, the condensate loading due to heat loss should not represent a significant problem for steam purity.

5.7 Potential Cause 6: Localised mineral deposits in the turbine seals.

As reported by the O&M team and evidenced by Figure 6 and Figure 7, the mineral deposits seem to be localised mainly in a segment of the turbine seals, and scaling problems in other parts of the turbine have not been reported. This situation appears abnormal and requires further investigation. A potential reason might be the injection of wet steam, specifically in that section of the turbine seals.

6. RECOMMENDATIONS

Based on the modelling results and the root cause analysis above presented, our recommendations are as follows:

- Validate the model results through more stable and accurate data gathering and considering the likely scenario of wells combination or production configuration.
- Carry out a separation efficiency measurement of the entire steamfield through a total chloride or sodium mass balance from the separators to the demisters.
- Improve the condensate trapping of the steam branch line TR-2/9. Figure 17 shows the concept of a proposed modification.
- Investigate in detail the reason for localised mineral deposits, specifically in a section of the turbine seals.
- Implement the measurements, modelling and preferred modifications before the next U2's overhaul, which is scheduled in February 2022.

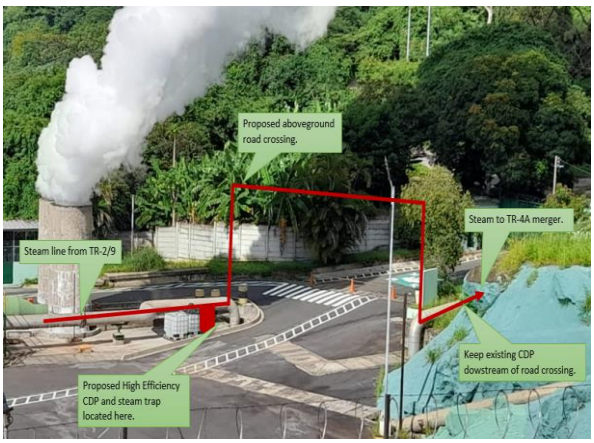

Figure 17 - Proposed modification on TR-2/9 steam branch line.

ACKNOWLEDGEMENTS

The authors would like to thank the staff and friends at LaGeo S.A. de C.V. for their interest in contributing to this technical paper's preparation.

The project was sponsored by the New Zealand Ministry of Business, Innovation and Employment (MBIE) through the Empowering Geothermal Energy project funds.

REFERENCES

ASTM C680-19. (2019). *Standard Practice For Estimate of the Heat Gain or Loss and the Surface Temperatures of Insulated Flat, Cylindrical, and Spherical Systems by Use of Computer Programs.* West Conshohocken, PA: ASTM.

Baker, O. (1954). Simultaneous Flow of Oil and Gas. *Oil and Gas Journal*, 185-195.

Bloch, H. P., & Geitner, F. K. (1999). *Practical Machinery Management for Process Plants.* Houston, Texas: Gulf Publishing Company.

Holmgren, M. (n.d.). *IAPWS IF-97 Water Thermodynamic Properties*. Retrieved from X-eng.com.

LaGeo. (2019). *Separation Efficiency and Steam Purity - Annual Report 2019.* San Salvador: Internal Report.

LaGeo. (2021). *Daily Production Report.* Berlin: Internal Report.

Lazalde-Crabtree, H. (1984). Design Approach of Steam-Water Separators and Steam Dryers For Geothermal Applications. *Geothermal Resources Council Bulletin*, 11-20.

Lee, K. (1980). Performance Tests of the Condensate Drain Pots at Wairakei. *Ministry of Energy, Electricity Division*.

Mills, T., & Lovelock, B. (2020). Geothermal Steam Purity Modelling - Theory And Practice. *Proceedings 42nd New Zealand Geothermal Workshop, 24-26 November 2020, Waitangi, New Zealand*.

Morris, C. J., Mroczek, E. K., & Misa, T. N. (2019). Geothermal steam condition performance monitoring. *Geothermics*.

Morris, C., & Mroczek, E. (2015). Turbine Scaling. *Proceedings the 37th New Zealand Geothermal, 18-20 November, Taupo, New Zealand.*

Rennels, D. C., & Hudson, H. M. (2012). *Pipe Flow - A Practical and Comprehensive Guide.* Hoboken, New Jersey: John Wiley & Sons, Inc.

Zarrouk, S. J., & Purnanto, M. H. (2014). Geothermal steam-water separators: Design overview. *Geothermics*.

ISSN 2703-4275